Covalent bonds and their crucial effects on pseudogap formation in α-Al(Mn,Re)Si icosahedral quasicrystalline approximant

K. Kirihara,[1,2,*] T. Nagata,[3] K. Kimura,[2,3] K. Kato,[4] M. Takata,[5] E. Nishibori,[5] and M. Sakata[5]
[1]*Intelligent Modeling Laboratory, University of Tokyo, 113-8656 Tokyo, Japan*
[2]*Department of Advanced Materials Science, University of Tokyo, 113-0033 Tokyo, Japan*
[3]*Department of Materials Science, University of Tokyo, 113-8656, Japan*
[4]*Japan Synchrotron Radiation Research Institute, 679-5198 Hyogo, Japan*
[5]*Department of Applied Physics, Nagoya University, 464-8603 Nagoya, Japan*
(Received 3 December 2002; revised manuscript received 18 February 2003; published 31 July 2003)

X-ray charge densities of Al-based icosahedral quasicrystalline approximant crystals α-AlReSi, α-AlMnSi, and $Al_{12}Re$ were observed by a combination of the maximum entropy method with the Rietveld method. We successfully obtained the clear images of interatomic covalent bonds between Al and transition metals (Mn, Re) and those in the Al (or Si) icosahedron in Mackay icosahedral clusters of both α-AlReSi and α-AlMnSi approximant crystals. The bonding nature of the three kinds of glue atom sites connecting Mackay icosahedral clusters was also clarified. This covalent bonding nature should strongly relate with the enhancement of the electron density-of-states pseudogap near the Fermi level. In addition, the interatomic covalent bonds of α-AlReSi are stronger than those of α-AlMnSi. This fact leads to the low effective carrier density of α-AlReSi in comparison with that of α-AlMnSi. Unlike the covalent bonding nature of an icosahedron in α-AlReSi and α-AlMnSi crystals, the Al icosahedron with an Re center atom exhibits no Al-Al interatomic covalent bonds in the $Al_{12}Re$ crystal. The tendency for metallic-covalent bonding conversion in the Al icosahedron, which is related to the atom site occupancy of the icosahedral cluster center, is also strongly supported.

DOI: 10.1103/PhysRevB.68.014205 PACS number(s): 71.23.Ft, 61.10.Nz, 61.44.Br

I. INTRODUCTION

A question about the origin of semiconductorlike electron transport in Al-based icosahedral quasicrystals is still open, even though much research has already taken place. The semiconductorlike properties arise from the icosahedral symmetry and the quasiperiodic structure, and can be explained by the combination of a Hume-Rothery pseudogap in the electron density of states (DOS) at the Fermi level, $N(E_F)$, and a localization tendency of electrons near E_F.[1] At low temperature below 300 K, the theory of quantum interference effects based on weak localization and electron-electron interaction qualitatively provided a reasonable explanation for temperature or magnetic field dependencies of the electrical conductivity in many Al-based quasicrystalline alloys.[2] However, another experimental fact, that the electrical conductivity and its temperature coefficient exhibit strong composition dependence[3–5] and also depend strongly on the difference in alloy systems,[6] remains to be explained.

The electrical resistivity, ρ, (conductivity, σ) can be given by $\rho\ (=1/\sigma)=1/e^2DN(E_F)$, where D is the diffusivity of the carrier. AlPdRe quasicrystals possess the highest electrical resistivity (the lowest electrical conductivity) values among all of the reported Al-based icosahedral quasicrystals.[7–11] On the other hand, Guo *et al.* and Fisher *et al.* have recently reported the large difference in the resistivities at room temperature, ρ_{RT}, between arc-melted polygrain samples (6250–16 000 $\mu\Omega$ cm) and the structurally very perfect single grain ones (1500–3200 $\mu\Omega$ cm) for the AlPdRe quasicrystal,[12,13] which means the origin of the highest resistivity should be partly the effect of grain boundary, which should reduce the value of D. Fisher *et al.* prepared single grains of both AlPdRe (Ref. 13) and AlPdMn (Refs. 14 and 15) quasicrystals by the same self-flux method. The values of ρ_{RT} of these ''flux-grown'' samples are 1500–3200 $\mu\Omega$ cm for the AlPdRe system[13] and 1570 $\mu\Omega$ cm (Ref. 14) and 1200 $\mu\Omega$ cm (Ref. 15) for the AlPdMn system. The maximum value of ρ_{RT} for AlPdMn never exceeds that of AlPdRe. This fact should be explained by the difference in $N(E_F)$ related to the covalent bonding nature of quasicrystals and approximants. The deep pseudogap causes the low $N(E_F)$ value and, in other words, the low effective carrier density. The value of $N(E_F)$ is proportional to that of the electronic specific-heat coefficient, γ. The AlPdRe quasicrystals possess lowest values of γ (<0.11 mJ/mol K^2)[11,16] in comparison with other non-Re-containing quasicrystals (0.11–0.41 mJ/mol K^2).[2] The measurement of specific heat itself has no relation to the problems of grain boundaries. Therefore, the correlation between ρ_{RT} and γ, i.e., $N(E_F)$, which has been frequently indicated,[2] seems to be valid for the arc-melted polygrain Al-based quasicrystalline samples and for the single grain ones, respectively.

It has been frequently discussed that the Hume-Rothery pseudogap is due to a Fermi-surface Jones zone (FS-JZ) interaction. This interaction is enhanced when the Fermi-sphere diameter $2k_F$ matches the wave number of the intense Bragg peak K_p. The value of $2k_F$ can be estimated from the sp valence electrons per atom (e/a) ratio. One may compare this rule to the Hume-Rothery matching rule. The Hume-Rothery picture applies to a nearly-free-electron system in which the potential for the valence electron is rather weak. For example, this picture is solely applied to the case of the AlMgZn quasicrystal, as Sato *et al.* clarified by the band-structure calculation for the AlMgZn approximant crystal.[17] On the other hand, Al-transition-metal (TM) quasicrystalline alloys possess larger values of resistivity and temperature

 ©2003 The American Physical Society

coefficient than the quasicrystalline alloys containing no TM's. It has been widely adopted that the Al-TM quasicrystals obey the Hume-Rothery matching rule by imposing negative e/a values on TM's,[18] and thus the FS-JZ interaction still occurs. However, those effects are not enough to explain the large variation in resistivity, Hall coefficient, and thermoelectric power with a slight change of TM concentration. First-principles band-structure calculations indicated the importance of an orbital hybridization between the Al sp band and the TM d band for approximant crystals of the Al-TM quasicrystals[19–21] and other Al-TM Hume-Rothery alloys.[22,23] In addition, Belin *et al.* also reported sp-d hybridization by soft-x-ray emission or absorption spectroscopy for various Al-TM quasicrystals and approximants.[24,25] This means that a combination of the FS-JZ interaction and the sp-d hybridization is required to consider the enhancement of the DOS pseudogap. However, these calculations and spectroscopy studies have not been able to reveal a definite contribution of individual atoms to the pseudogap formation, because of the complex atomic structure. Hence, the relation between unique electrical properties and atomic structure is still not clearly understood.

We have stressed a strong dependence of electrical conductivity on the difference in alloy systems for Al-based quasicrystals and approximants, and have discussed the relation between electrical properties and local atomic structure.[6,26] Charge-density studies give direct evidence for interatomic bonds and thus provide a better understanding of the relation of nonmetallic properties with local atomic structure. Since accurate atomic structure analysis is difficult because of the lack of structural periodicity, analyzing the charge density is quite difficult for quasicrystals. However, we could obtain the charge density for approximant crystals. The structure of the approximant crystals can be described, in most cases, as a periodic arrangement of the icosahedral cluster, e.g., the Mackay icosahedral (MI) cluster[27] or Bergman cluster.[28] Both types of icosahedral clusters are considered to be the basic space-filling units of icosahedral quasicrystals. Detailed research on the electrical properties of the approximants have clearly shown that 1/1-cubic approximants such as the α-AlMnSi phase[29] and the α-AlCuFeSi phase[30] possess quasi-crystalline-like electrical properties. Higher-order approximants greater than the 1/1-cubic approximant also possess nonmetallic behavior. Recently, Mizutani *et al.* summarized the results of their study on a large number of 1/1-cubic approximant crystals including the above approximants.[31] They reported that the electrical properties of the approximant crystals also reveal strong dependence on the difference in alloy systems. With *ab initio* band-structure calculations of the α-AlMn(Si) approximant crystal, Fujiwara reported that the hybridization between Al sp band and Mn d band enhances the pseudogap and then stabilizes the MI clusters and their cubic packing.[19] Recently, Tamura *et al.* reported the composition dependence of the electrical conductivity of the α-AlReSi 1/1-approximant,[32] which is isostructural to α-AlMnSi. They also reported that α-AlReSi reveals the highest value of resistivity among all the approximant crystals.[33] Although the AlPdRe approximant crystal itself has not been found yet, the charge density of the α-AlReSi crystal should clarify the role of the Re atoms on the nonmetallic behavior of not only the α-AlReSi crystal but also the AlPdRe quasicrystal in view of the DOS pseudogap feature. Hence, even the bonding nature in the 1/1-approximant crystals should reveal an important factor dominating the nonmetallic behavior.

The maximum entropy method (MEM) used along with Rietveld analysis is a powerful method for obtaining a clear image of the charge density. Takata *et al.* developed this method[34] and successfully obtained the bonding electron images for fullerene compound,[35] the α-rhombohedral boron (B) crystal,[36] manganese oxide,[37] magnesium diboride,[38] etc. Previously, we also reported the x-ray charge density of α-AlMnSi and $Al_{12}Re$ using this method, and clearly showed the existence of covalent bonds in the MI cluster in α-AlMnSi.[39] Covalent bonds in the MI cluster were found to play a crucial role in nonmetallic properties of α-AlMnSi. In this paper, we report on clearer charge densities of α-AlMnSi and $Al_{12}Re$ than those shown with previous data. In addition, the charge density of the highest resistive α-AlReSi is presented and compared to that of the above two approximants. We discuss how the bonding nature of the MI clusters and the glue atoms, which connect the MI clusters, relates with the FS-JZ interaction and sp-d hybridization. The charge transfer between Al and TM's frequently revealed by some researchers[22,49,50] is also discussed.

II. EXPERIMENT AND ANALYSIS

Ingots of $Al_{72.5}Re_{17.5}Si_{10}$, $Al_{72}Mn_{16}Si_{12}$, and $Al_{12}Re$ alloys were prepared from elemental constituents $(3N–4N)$ by arc melting under an Ar atmosphere. Sample homogenization of Al-Re-Si alloy and Al-Mn-Si alloy ingots was achieved by postinductive melting, after which single-phase bulk samples were prepared by annealing the ingots at 1073 K for 48 h and 953 K for 17 h under an Ar atmosphere for α-AlReSi and α-AlMnSi, respectively. Al-Re alloy ingots were placed in an evacuated quartz tube and heated to 923 K, which is slightly below the peritectic point, and held for 5 h. The Al-Re samples were then cooled to 875 K over 16 h to obtain single-phase bulk samples of the $Al_{12}Re$ crystalline phase. The electrical resistivity was measured by the van der Pauw method in the temperature range from 50 K to 295 K. Remainders of these ingots were carefully ground into powder so that they did not reveal any preferred orientation. Powder x-ray-diffraction (XRD) patterns were collected at room temperature using a large scale Debye-Scherrer camera installed at the Spring-8 synchrotron-radiation facility, beamline BL02B2.[40] By choosing the wavelength to be 0.5 Å for α-AlReSi and $Al_{12}Re$ and 0.8 Å for α-AlMnSi, and the diameter of glass capillary to be 0.2 mm, no correction to x-ray absorption was required in the measured 2θ range. An imaging plate (IP) was used as a detector. Exposure time was 1 h for α-AlReSi and $Al_{12}Re$, and 3 h for α-AlMnSi so that dynamic range of the sensitivity of the IP was fully employed to obtain the XRD patterns with good statistics. The powder XRD pattern was obtained with 0.01° in 2θ for all the samples.

For the pre-Rietveld analysis, we chose the crystal struc-

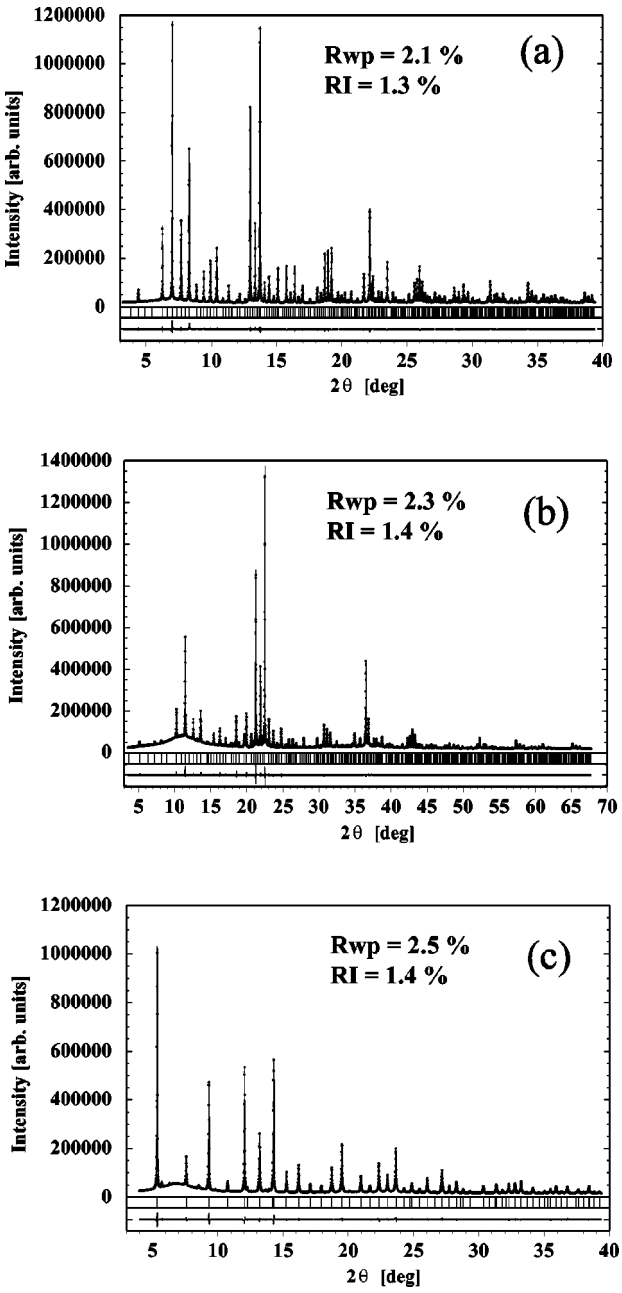

FIG. 1. Rietveld fitting results for (a) α-AlReSi, (b) α-AlMnSi, and (c) $Al_{12}Re$.

ture of α-AlMnSi and $Al_{12}Re$ reported in Ref. 41 as the initial structure models. As mentioned above, α-AlReSi is isostructural with α-AlMnSi and thus the α-AlReSi crystal structure can be constructed by replacing Mn atoms in α-AlMnSi with Re atoms.[32] Figure 1 shows the XRD patterns and the fitting results of the pre-Rietveld analysis of [Fig. 1(a)] α-AlReSi, [Fig. 1(b)] α-AlMnSi, and [Fig. 1(c)] $Al_{12}Re$. Reasonably low values of reliability factors shown in Fig. 1 reveal that good fitting results are obtained for all the samples. The observed structure factors were then extracted from raw XRD patterns using the results of the pre-Rietveld analysis as a reference. Numbers for the observed structure factors were 832, 749, and 92 for α-AlReSi, α-AlMnSi, and $Al_{12}Re$, respectively. And the resolution in d spacing was 0.802 Å, 0.820 Å, and 0.802 Å for α-AlReSi, α-AlMnSi, and $Al_{12}Re$, respectively. The charge density derived from the MEM analysis is consistent with these observed structure factors and is least biased with unobserved structure factors. Thus the charge density corresponding to the bonding electrons can be reasonably derived. Takata *et al.* recently explained the detailed principle of the MEM elsewhere.[34] A computer code ENIGMA (Ref. 42) was employed with the MEM analysis with $128\times128\times128$, $126\times126\times126$, and $76\times76\times76$ pixels per cubic lattice, for α-AlReSi, α-AlMnSi, and $Al_{12}Re$, respectively. The reliability factors of the final MEM charge density were 2.2%, 1.7%, and 1.0% for α-AlReSi, α-AlMnSi, and $Al_{12}Re$, respectively. According to these results, we obtained the bonding electron images of the approximant crystals.

III. CRYSTAL STRUCTURES AND CHARGE DENSITIES

We summarize the crystal data and the refined structural parameters of the three samples in Table I. The crystal structures are drawn in Fig. 2. Both α-AlMnSi and α-AlReSi have bcc packing of the MI clusters and the glue atom sites, which are inserted between the MI clusters. The atom sites of the MI cluster at origin (O) and body (B) center are labeled O1, O2x and B1, B2x (x=a, b, c), respectively. The three kinds of glue atom sites are labeled M2, M5, and M7, referring to Ref. 41. Since one of the glue atom sites (M2) breaks the bcc packing symmetry, both crystalline phases exhibit the space group $Pm\bar{3}$ (number 200). The pre-Rietveld analysis indicated that the atom species and occupancy of the MI cluster first shell centered at the origin of unit cell are slightly different from those of the first shell centered at the body center. However, it should be noticed that we couldn't easily distinguish the Al atom from the Si atom from the pre-Rietveld analysis, since the difference in x-ray scattering intensity between Al (Si) and Re was much larger than that between Al and Si. The resultant structures of α-AlMnSi and $Al_{12}Re$ are almost the same as those reported in our previous paper.[39]

Figure 3 shows the equidensity surfaces of the charge density (0.35 $e/Å^3$) of the MI cluster in the α-AlReSi crystal. The MI cluster centered at the origin of the unit cell is shown. The Al-Al interatomic covalent bonds in the Al icosahedron (first shell: O1 site) and the Al-Re interatomic covalent bonds in the second shell (Al:O2a and O2b sites; Re: O2c site) can be clearly seen. In the case of the MI cluster at the body center, the interatomic charge-density distribution of the first shell [B1 site shown in Fig. 4(a)] apparently indicates a cubic symmetry. The Al-Re interatomic covalent bonds in the second shell [Al: B2a and B2b sites, Re: B2c site shown in Fig. 4(b)] are weaker than those of the MI cluster at the origin but a similar covalent bonding nature is revealed at the low-density level [0.30 $e/Å^3$, Fig. 4(c)].

We additionally obtained images of the Al-Re interatomic covalent bonds between Al atoms in the MI cluster first shell (O1 or B1 site) and the Re atoms in the MI cluster second shell (O2c or B2c site). They can be seen in the section

TABLE I. Crystal data and refined structural parameters for α-AlReSi, α-AlMnSi, and $Al_{12}Re$. Parentheses in site names refer to the crystallographic data of Al_9Mn_2Si in Ref. 41. In the previous paper, we used the site name of (O1, B1), (O2a, O2b, B2a, B2b), (O2c, B2c), (M5, M7), and M2 for A1, A2, Mn, G1, and G2 in AlMnSi, respectively (Ref. 39). g is the occupancy at each atomic site. B is a thermal parameter.

Site	Wyckoff	Atom	g	x	y	z	B (Å^2)
			α-AlReSi				
			$Pm\bar{3}$, a=12.88224(1) Å				
O1(M4)	12j	Al	0.972(7)	0	0.1623(5)	0.0983(5)	0.65(4)
O2a(M1)	6e	Al	0.95(1)	0.3662(5)	0	0	0.50(7)
O2b(M8)	24l	Al	0.975(4)	0.1204(3)	0.1887(4)	0.3012(3)	0.69(3)
O2c(Mn1)	12j	Re	1.0	0	0.32456(4)	0.19845(4)	0.506(7)
B1(M6)	12k	Al	0.35(22)	1/2	0.3393(5)	0.4009(5)	0.65(4)
		Si	0.65(22)				
B2a(M3)	6h	Al	0.98(2)	0.1167(5)	1/2	1/2	0.50(7)
B2b(M9)	24l	Al	0.967(9)	0.3900(3)	0.3127(4)	0.1923(3)	0.69(3)
B2c(Mn2)	12k	Re	1.0	1/2	0.18023(6)	0.30472(8)	0.47(2)
M2(M2)	6f	Al	0.82(15)	0.2984(4)	0	1/2	0.39(9)
		Si	0.18(15)				
M5(M5)	12j	Al	0.955(9)	0	0.3268(2)	0.4036(3)	0.54(6)
M7(M7)	12k	Al	1.0	1/2	0.1229(2)	0.1102(3)	0.54(6)
			α-AlMnSi				
			$Pm\bar{3}$, a=12.66126(1) Å				
O1(M4)	12j	Al	0.62(3)	0	0.1669(2)	0.1010(2)	0.61(2)
		Si	0.38(3)				
O2a(M1)	6e	Al	1.0	0.3662(2)	0	0	0.66(3)
O2b(M8)	24l	Al	1.0	0.1181(1)	0.1886(1)	0.2985(1)	0.67(1)
O2c(Mn1)	12j	Mn	1.0	0	0.32715(7)	0.19827(7)	0.48(2)
B1(M6)	12k	Al	0.44(3)	1/2	0.3363(2)	0.3996(2)	0.61(2)
		Si	0.56(3)				
B2a(M3)	6h	Al	1.0	0.1245(2)	1/2	1/2	0.66(3)
B2b(M9)	24l	Al	1.0	0.3908(1)	0.3132(1)	0.1962(1)	0.67(1)
B2c(Mn2)	12k	Mn	1.0	1/2	0.17916(9)	0.3076(1)	0.43(2)
M2(M2)	6f	Al	0.37(5)	0.2888(2)	0	1/2	0.70(4)
		Si	0.63(5)				
M5(M5)	12j	Al	1.0	0	0.3310(2)	0.4022(2)	0.69(2)
M7(M7)	12k	Al	1.0	1/2	0.1230(2)	0.1172(2)	0.69(2)
			$Al_{12}Re$				
			$Im\bar{3}$, a=7.52809(1) Å				
Re	2a	Re	1.0	0	0	0	0.31(1)
Al	24g	Al	1.0	0	0.1879(1)	0.3082(1)	0.68(1)

contour maps of the (100) plane and the (200) plane shown in Figs. 5(c) and 5(d), respectively. The O1-O2c and B1-B2c bonds correspond to termination of sticking covalent bonds along fivefold axes of Al (Si) icosahedrons. These O1-O2c and B1-B2c interatomic bonds are the strongest covalent bonds in this crystal. Glue atoms M2, M5, and M7 are also strongly bonded to Re atoms. As seen in the (100) plane, the Al (Si) atom at the M2 site and the Al atom at the M5 site are bonded to the Re atom at the O2c site. The direction of the M2-O2c interatomic bonds coincides with that of O1-O2c interatomic bonds, which indicate fivefold axes of the MI cluster. The Al (Si) atom at the M2 site connects the MI clusters at two adjacent unit cells along the $\langle 010 \rangle$ direction by terminating two M2-O2c interatomic bonds. The Al atom at the M5 site is bonded not only to the O2c site but also to be M5 site in the adjacent unit cell. In addition, we found the Al-Re interatomic bonds between M5 and B2c sites. This means that the M5 site connects the MI clusters along both the $\langle 100 \rangle$ direction and $\langle 111 \rangle$ direction and plays the most important role as the ''glue atom.'' The Al atom at the M7 site is bonded to the Re atom at B2c site only, and does not contribute to the connection of the MI clusters.

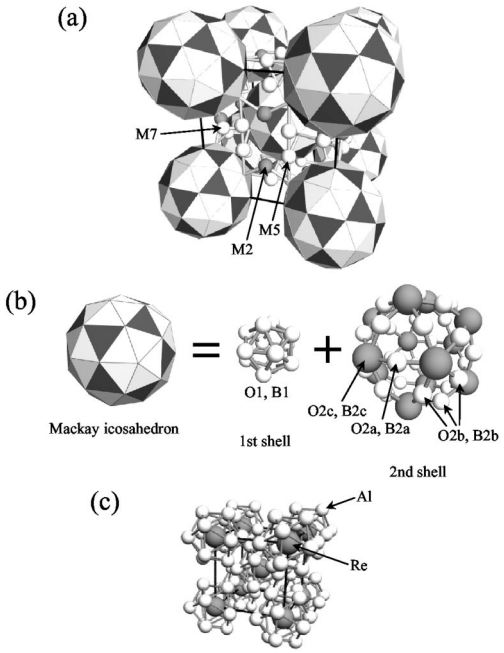

FIG. 2. (a) Crystalline structures of α -AlReSi and α -AlMnSi. (b) Structure of the Mackay icosahedral cluster. (c) Crystalline structure of $Al_{12}Re$.

The charge-density section contour maps of the (100) plane and the (200) plane in the α-AlMnSi crystal are shown in Figs. 6(a) and 6(b), respectively. Common features in the bonding nature of α-AlMnSi are very similar to those of previous results[39] and those presented here for α-AlReSi. However, charge densities of interatomic bonds of α-AlMnSi are much smaller, i.e., the bonds are weaker than those of α-AlReSi.

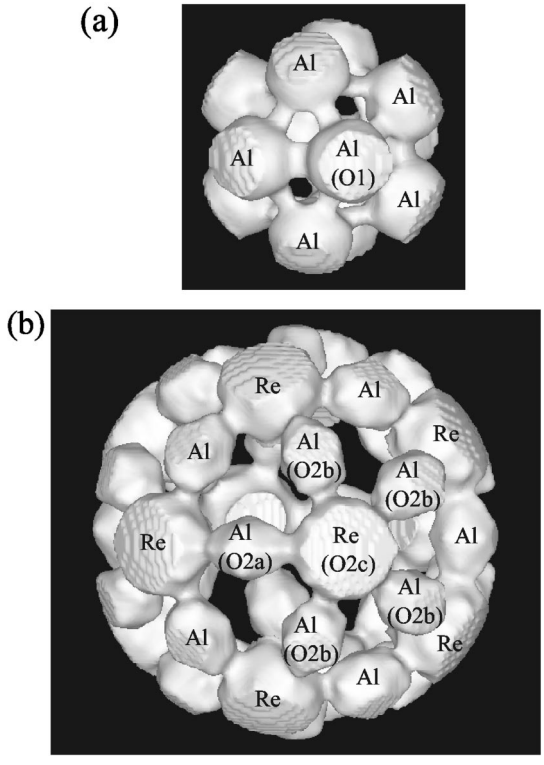

FIG. 3. Equidensity surfaces of charge density of the Mackay icosahedral cluster in α-AlReSi. The cluster is positioned at the origin of the unit cell. (a) First shell. (b) Second shell. Electron density at surfaces is 0.35 $e/Å^3$.

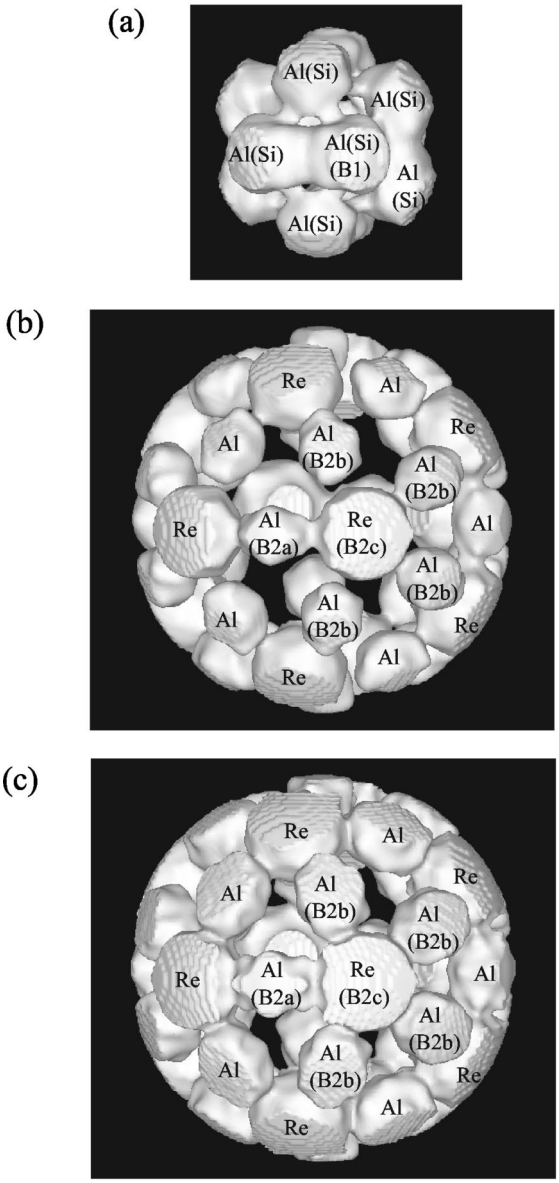

FIG. 4. Equidensity surfaces of charge density of the Mackay icosahedral cluster in α-AlReSi. The cluster is positioned at the body center of the unit cell. (a) First shell. (b) and (c) Second shell. Electron density at surfaces is 0.35 $e/Å^3$ for (a) and (b), and 0.30 $e/Å^3$ for (c), respectively.

Figure 7 shows the equidensity surface of the charge density [Fig. 7(a) is 0.35 $e/Å^3$ and Fig. 7(b) is 0.30 $e/Å^3$] for $Al_{12}Re$. Note that no interatomic covalent bond exists between Al atoms of the 13-atom icosahedral cluster with the central Re atom. This characteristic is quite different from the interatomic-Al covalent bonds of the 12-atom icosahedron without the center atom in α-AlReSi. This result can also be clearly seen in the charge-density section contour maps of the (200) plane in $Al_{12}Re$ shown in Fig. 8.

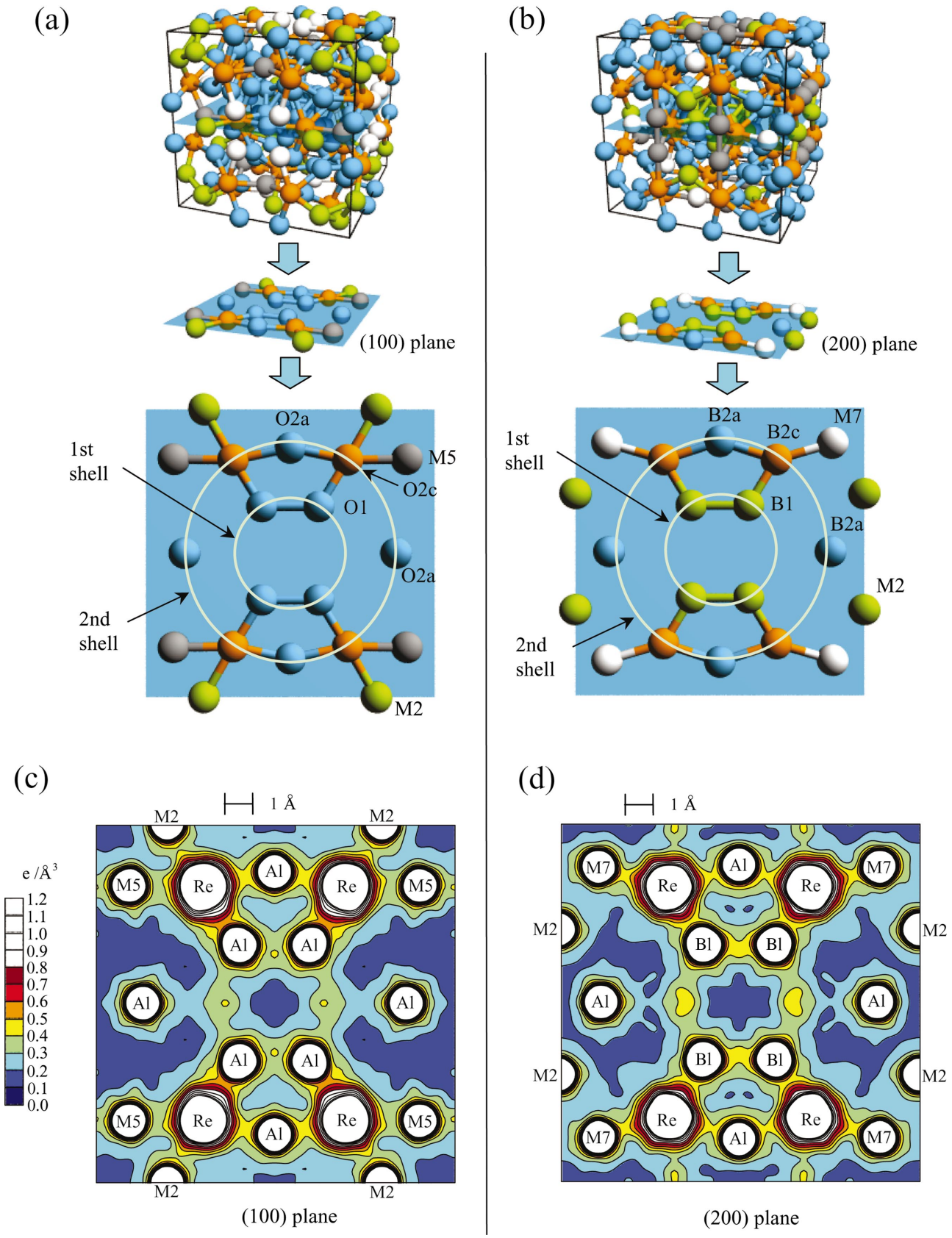

FIG. 5. (Color) Crystal structure and section contour maps of charge density of α-AlReSi in the range of 0.00–1.20 $e/\text{Å}^3$ with a step of 0.10 $e/\text{Å}^3$. The contour maps in the range of 0.00–0.80 $e/\text{Å}^3$ are colored. (a) and (c) (100) plane. (b) and (d) (200) plane.

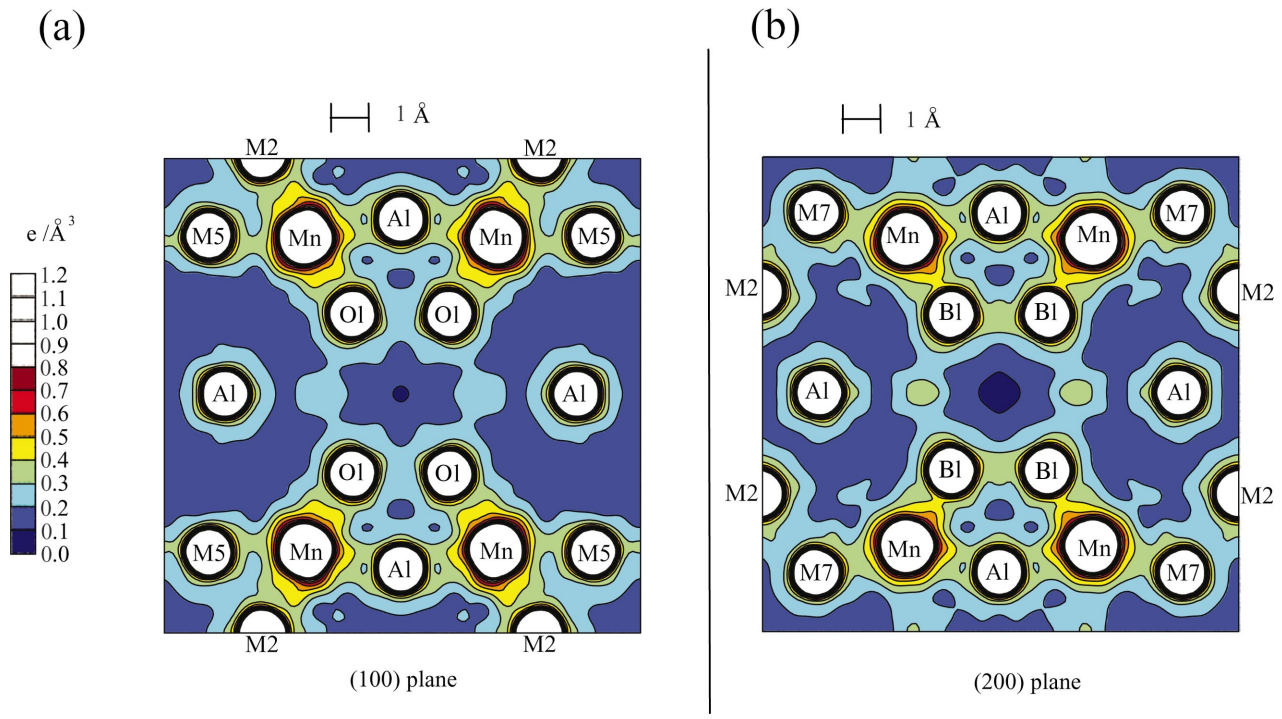

FIG. 6. (Color) Section contour maps of charge density for α-AlMnSi in the range of 0.00–1.20 $e/\text{Å}^3$ with a step of 0.10 $e/\text{Å}^3$. The contour maps in the range of 0.00–0.80 $e/\text{Å}^3$ are colored. (a) (100) plane. (b) (200) plane.

IV. DISCUSSION

It is important to mention the comparison between our charge-density results and *ab initio* calculations or any other spectroscopic experiments. Recently, Onogi *et al.* reported the result of Rietveld analysis and band calculations using a linear muffin-tin orbital method for α-AlReSi.[43] However, they presented no information about bonding or hybridization so far. It is meaningful to compare our data with the similar band calculation for α-AlMn(Si) since Fujiwara reported the detailed electronic structure of α-AlMn, in which Si atoms in α-AlMnSi were replaced by Al.[19] He found that the Mn $3d$ band is split at its middle near E_F and that the binding peak of DOS is slightly below E_F. This binding peak is mainly due to the local projected DOS of the Mn d state, the Al p state of first shell, and the second shell of the MI cluster. The pseudogap was clearly revealed near E_F in the total DOS curve. Hence it was supposed that the orbital hybridization between the Al p state and the Mn d state strongly contributes to the pseudogap formation. Although difference occurs when Si atoms are included in the crystal or not, the covalent bonding nature in the MI cluster mentioned in the previous section agrees well with the calculation results of Fujiwara. Belin *et al.* performed soft-x-ray emission and absorption spectroscopy measurements for various Al-Mn compounds including the Al_6Mn crystal, the Al_6Mn icosahedral quasicrystal, and the Al_4Mn decagonal quasicrystal.[24] They also showed that in the Al_6Mn crystal and the icosahedral quasicrystal, the hybridization between the Al $3s$ and $3p$ bands and Mn $3d$ band is responsible for the opening in the pseudogap near E_F. This orbital hybridization is viewed as the Al(Si)-Mn covalent bonds in our-

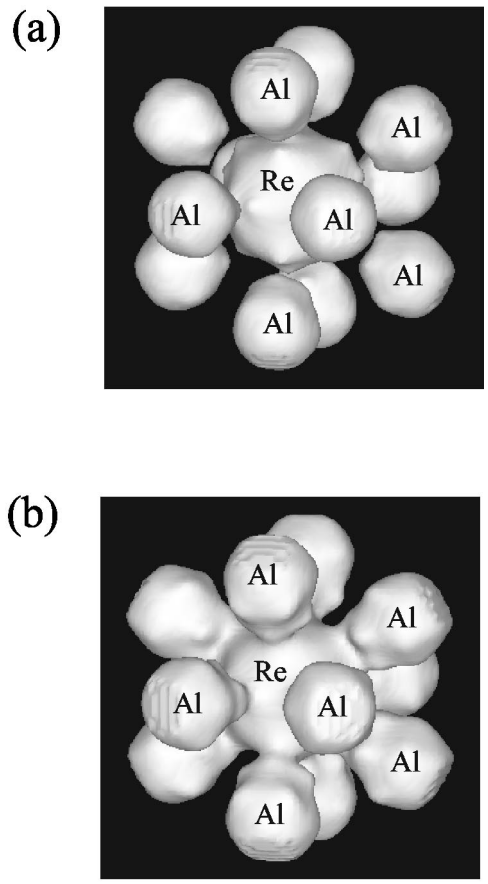

FIG. 7. Equidensity surfaces of charge density of 13-atom icosahedron in $Al_{12}Re$. Electron density at surfaces is 0.35 $e/\text{Å}^3$ for (a), and 0.30 $e/\text{Å}^3$ for (b).

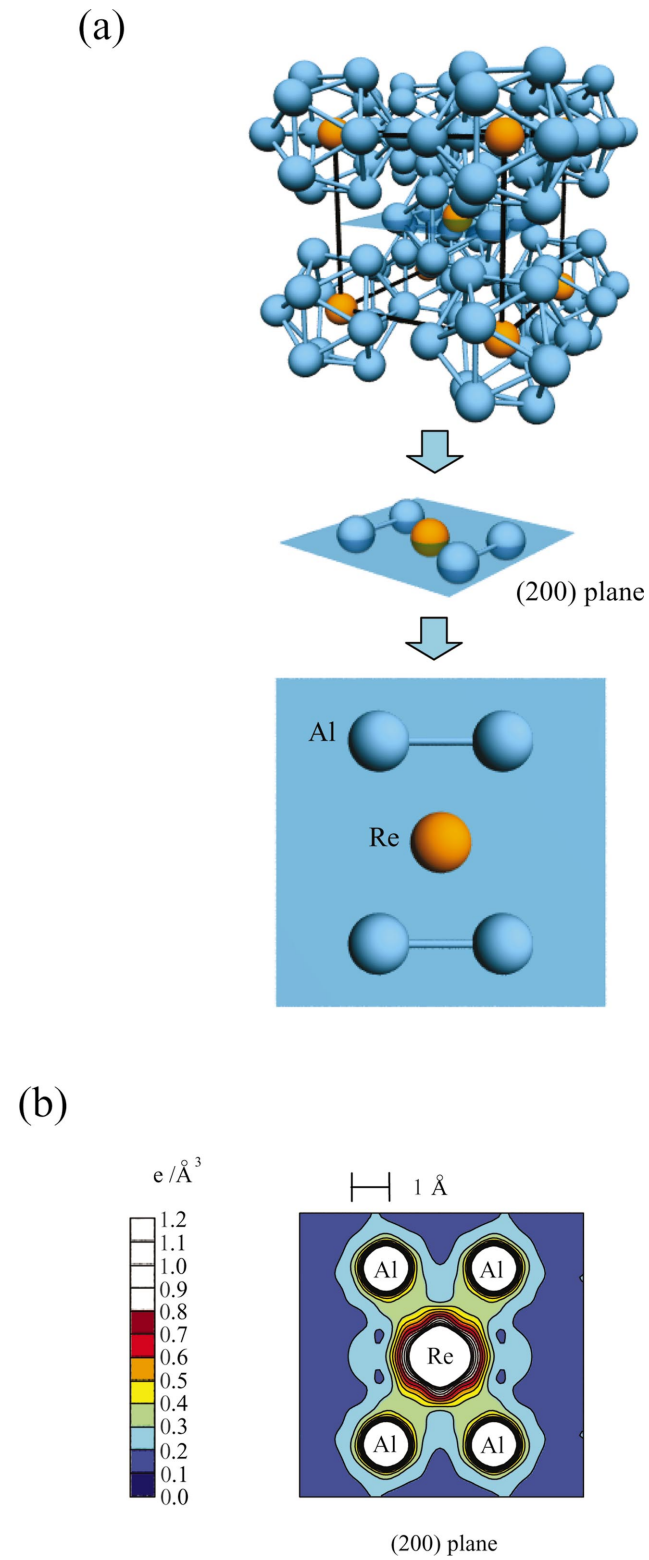

FIG. 8. (Color) Crystal structure (a) and section contour maps (b) of (200) plane charge density of $Al_{12}Re$ in the range of 0.00–1.20 $e/Å^3$ with a step of 0.10 $e/Å^3$. The contour maps in the range of 0.00–0.80 $e/Å^3$ are colored.

study. Although the charge-density value of the interatomic bond of α-AlMnSi is smaller than that of α-AlReSi, distributions of covalent bonds are entirely similar to each other. Onogi *et al.* presented the total DOS of α-AlReSi and showed a pseudogap structure near E_F, which is very similar to the case of α-AlMn.[43] The clear Al(Si)-Re interatomic covalent bonds shown in Figs. 3–5 also correspond to the real-space images of the hybridization characteristics between the Al $3s$ and $3p$ band and the Re $5d$ band.

By estimating $2k_F$ from the e/a values, we found that $2k_F$ values of both α-AlReSi and α-AlMnSi approximants are quite close to K_p of the intense (530) peak and (523) peak with a multiplicity of 12 and 24, respectively. Both approximants seem to obey the Hume-Rothery matching rule. It should be noted that Fermi spheres of both α-AlReSi and α-AlMnSi interact exactly with the same Jones zone and thus a difference in the degree of the FS-JZ interaction between these approximants hardly exists. However, interatomic covalent bonds of α-AlMnSi are much weaker than those of α-AlReSi, as described above. This result apparently arises from the difference in the degree of the sp-d hybridization between Al sp electrons and TM d electrons. We can see this difference in more detail by the charge density at bond midpoint (CDBM) shown in Fig. 9. The CDBM of Al(or Si)-Re interatomic bonds in α-AlReSi are larger than those of Al(or Si)-Mn interatomic bonds in α-AlMnSi [Fig. 9(a)]. The $5d$ electrons of Re have a stronger hybridization effect or bonding effect than the $3d$ electrons of Mn. Recently, Krajčí and Hafner calculated the electronic structure of Al_2TM (TM=Fe, Ru, Os) compounds.[44] They reported that the band gap of the compounds becomes wider if a $3d$ (Fe) metal is replaced by a $4d$ (Ru) or $5d$ (Os) metal. Hence, the increasing covalent character in $5d$ transition metals also seems to have crucial effects on the case of α-AlReSi. In addition, it was found that the CDBM of Al(or Si)-Al (or Si) interatomic covalent bonds in α-AlReSi is also larger than those in α-AlMnSi [Fig. 9(b)]. The difference is evident for O1-O1 or B1-B1 interatomic bonds and for M5-M5 interatomic bonds. The reason for this fact is discussed in the next paragraph. The difference in the covalent character agrees with the difference in electrical resistivity between α-AlMnSi and α-AlReSi. The values of resistivity at 295 K are 3500 $\mu\Omega$ cm and 12 800 $\mu\Omega$ cm for α-AlMnSi and α-AlReSi, respectively. Although an examination with a scanning electron microscope revealed more porous structure for the α-AlReSi sample than the α-AlMnSi sample, the resistivity of α-AlReSi is larger than that of α-AlMnSi, to a large extent. These strong covalent bonds in α-AlReSi should explain the small number of effective carriers at E_F by the enhanced pseudogap and evidently lead to the higher electrical resistivity in comparison to that of α-AlMnSi. The above conclusion, that $N(E_F)$, i.e., γ, and resistivity at room temperature are smaller and higher, respectively, for α-AlReSi than for α-AlMnSi, has been confirmed by the recent systematic experiments of silicon content dependencies of the specific heat and electrical resistivity for melt-spun samples reported by Takeuchi *et al.*[45]

We now discuss the difference in the bonding natures of the 12-atom icosahedron without the center atom (MI first shell of α-AlReSi and α-AlMnSi) and the 13-atom icosahedron with the central Re atom ($Al_{12}Re$). Al-Al interatomic

covalent bonds observed for α-AlReSi and α-AlMnSi are absent in the 13-atom icosahedron of $Al_{12}Re$. The variation in the bonding nature of the icosahedral cluster agrees well with the fundamental characteristics derived by molecular-orbital (MO) calculations. Fujimori and Kimura[46] indicated with the MO calculation that even though the energy gain is sufficiently large for placing an atom at the center of a 12-atom icosahedron of Al and B, only a small gain is realized for an icosahedron having 12 hydrogen atoms, which terminate 12 dangling bonds sticking along fivefold axes. If a cluster exhibits a metallic bonding nature due to having an atom placed at its center, then such occupation would act to stabilize it. On the other hand, if the cluster is forced to have a covalent bonding nature because of its environment, then the center site should be empty. We reported this consideration previously by comparing the bonding natures of α-AlMnSi and $Al_{12}Re$.[39] The images of the Al(Si)-Al(Si) covalent bonds in α-AlReSi provide other clear evidence for the origin of the variation in the bonding nature of the Al(Si) icosahedron. The tendency for metallic-covalent bonding conversion in the Al icosahedron, which is related to the atom site occupancy of the icosahedral cluster center, is also strongly supported. In α-AlReSi and α-AlMnSi, the sticking bonds along fivefold axes of the icosahedron are considered to be terminated by Re and Mn atoms, respectively. Because the termination, i.e., the force for the icosahedron to have a covalent bonding nature, should be stronger for Re than for Mn, a difference in the CDBMs of α-AlReSi and α-AlMnSi in Fig. 9(b) mentioned in the previous paragraph may arise. Since in the above MO calculation the central atom was chosen to be the same as the atom of the icosahedron, such as Al or B, there is a difference in the atom species of the central atom in the $Al_{12}Re$. $Al_{12}Re$ is surmised to have metallic bonding but it exhibits weak hybridization in the Al atom of the icosahedron and the central Re atom. This weak hybridization may also contribute to the formation of the pseudogap. In fact, Carlsson performed the *ab initio* electronic structure calculations for a series of $Al_{12}W$-type crystals and then revealed the pseudogap formation for $Al_{12}Mn$ near E_F.[47] As described above, Trambly de Laissardiere *et al.* also reported a pseudogap formation in this compound.[22] However, this pseudogap is relatively shallower than that of α-AlReSi (Ref. 43) or α-AlMnSi.[19]

Examination of the atomic charge of each atom in the approximants is important because charge transfer from Al to transition metals has been frequently discussed. Yokoyama *et al.* reported that the Al-Cu-*TM* (*TM*=Fe, Ru, Os) quasicrystal and the Al-Pd-*TM* (*TM*=Mn, Re) quasicrystal could form at some specific composition area.[18] This composition area gives the specific e/a value of approximately 1.75, by taking the e/a value of the transition metal as negative value. Thus, the Hume-Rothery matching rule is believed to be effective for the Al-*TM* quasicrystal. The negative e/a value of transitionmetals was proposed by Pauling[48] and then first applied to various Al-*TM* alloys by Raynor.[49] The e/a value was indicated to be -4.66, -3.66, -2.66, -1.71, and -0.61 for Cr, Mn, Fe, Co, and Ni, respectively. Trambly de Laissardiere *et al.* calculated the band structure for a large number of Al-*TM* Hume-Rothery alloys and reported that

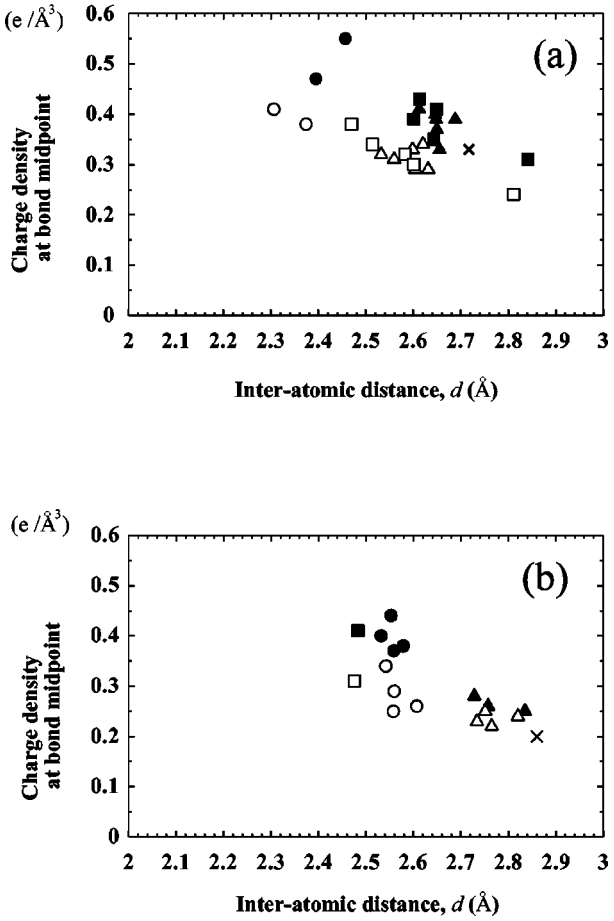

FIG. 9. Charge density at bond midpoint of interatomic bonds of (a) TM-Al (Si), and (b) Al (Si)-Al (Si). (a) The solid symbols represent the Re-Al (Si) interatomic bonds in α-AlReSi. The empty symbols represent the Mn-Al (Si) interatomic bonds in α-AlMnSi. The circles indicate O2c-O1 and B2c-B1. The triangles indicate O2c-(O2a,O2b) and B2c-(B2a,B2b). The squares indicate (O2c,B2c)-(M2,M5,M7). The cross symbol indicates Re-Al of $Al_{12}Re$. (b) The solid symbols represent the Al (Si)-Al (Si) interatomic bonds in α-AlReSi. The empty symbols represent the Al (Si)-Al (Si) interatomic bonds in α-AlMnSi. The circles indicate O1-O1 and B1-B1. The squares indicate M5-M5. The triangles indicate (O2a,O2b)-(B2a,B2b). The cross symbol indicates Al-Al of $Al_{12}Re$. The last two types of symbols (triangle and cross) do not indicate covalent bonds and are plotted for comparison with the covalent bonds (O1-O1, B1-B1, and M5-M5).

the negative valence of the transition metal is induced by the *sp-d* hybridization and its value agrees well with that proposed by Raynor.[22,50] This indicates the existence of an apparent charge transfer from Al to the transition metal. However, Krajčí *et al.* suggested that there exists no effective charge transfer indicated by *ab initio* band calculations of the Al-Pd-Mn approximant crystal, whose structure was hypothetically generated by a projection from six-dimensional space.[51] Our results revealed a small amount of charge transfer from Al to the transition metal for the MI second shell and two of the glue atom sites. Electron counts of each atom in the crystals studied were examined by the spherical integration of the charge density. The result is shown in Table II.

TABLE II. Electron counts of each atom in α-AlReSi, α-AlMnSi, and $Al_{12}Re$. $N(R_{ave})$ is the value of the spherical integration of the charge density whose radius is given by R_{ave}. R_{ave} indicates the average value of the distance between the atomic nucleus and the bond midpoint. R_{ave} is averaged over the coordination number, $n_{Al}+n_{TM}$, of the covalent bonds. n_{Al} and n_{TM} are the coordination numbers of each atom, which are covalently bound to Al(or Si) and the transition metal, respectively. N_{out} is the number of electrons, which are distributed to an outer region of each atom ($r>R_{ave}$) and is given by $N_{out}=N_a-N(R_{ave})$, where N_a indicates the total electron count of each atom estimated by multiplying the atomic number and site occupancy.

Site	n_{Al}	n_{TM}	R_{ave} (Å)	$N(R_{ave})$	N_{out}
			α-AlReSi		
O1(Al)	5	1	1.2(1)	11.6(6)	1.4(6)
O2a(Al)	0	2	1.0(1)	10.1(5)	2.9(5)
O2b(Al)	0	2	1.1(1)	10.6(5)	2.4(5)
O2c(Re)	8	0	1.6(1)	74(1)	1(1)
B1(Al+Si)	5	1	1.2(1)	12.2(6)	1.5(6)
B2a(Al)	0	2	1.1(1)	10.6(5)	2.4(5)
B2b(Al)	0	2	1.1(1)	10.6(5)	2.4(5)
B2c(Re)	9	0	1.6(1)	73(1)	2(1)
M2(Al+Si)	0	2	0.9(1)	10.2(5)	3.0(5)
M5(Al)	1	3	1.1(1)	11.1(6)	1.9(6)
M7(Al)	0	1	0.9(1)	9.7(4)	3.3(3)
			α-AlMnSi		
O1(Al+Si)	5	1	1.2(1)	11.8(5)	1.6(5)
O2a(Al)	0	2	1.0(1)	10.6(4)	2.4(4)
O2b(Al)	0	2	1.0(1)	10.6(4)	2.4(4)
O2c(Mn)	8	0	1.5(1)	25.5(7)	−0.5(7)
B1(Al+Si)	5	1	1.2(1)	12.0(5)	1.6(5)
B2a(Al)	0	2	0.9(1)	10.3(4)	2.7(4)
B2b(Al)	0	2	1.0(1)	10.7(4)	2.3(4)
B2c(Mn)	9	0	1.5(1)	25.3(7)	−0.3(7)
M2(Al+Si)	0	2	0.9(1)	10.9(3)	2.7(3)
M5(Al)	1	3	1.2(1)	11.5(5)	1.5(5)
M7(Al)	0	1	1.0(1)	10.7(3)	2.3(3)
			$Al_{12}Re$		
Al	0	1	1.1(1)	11.0(5)	2.0(5)
Re	12	0	1.7(1)	74.7(9)	0.3(9)

$N(R_{ave})$ is the value of spherical integration of the charge density whose radius is given by R_{ave}. R_{ave} indicates the average value of distance between atomic nucleus and bond midpoint. As shown in Figs. 5, 6, and 8, electrons of transition-metal atoms have a wider distribution range than those of Al(or Si) atoms. We define the bond midpoint for the Al(Si)-*TM* covalent bond as a point that has a minimum charge density along the covalent bond. $N(R_{ave})$ of Al(or Si) atoms of the MI second shell (O2a, O2b, B2a, and B2b) and the two glue atom sites (M2 and M7), which are only bonded to transition metal atoms ($n_{Al}=0$), are smaller than that of Al(or Si) atoms (O1 and B1), which are mainly bonded to Al(or Si) atoms ($n_{Al}>n_{TM}$). Inversely, the N_{out} of Al(or Si) atoms of O2a, O2b, B2a, B2b, M2, and M7 is larger than that of Al(or Si) atoms of O1 and B1. Therefore, we could see a sign of the charge transfer from Al to the transition metal for the valence electrons of the Al atom at O2a, O2b, B2a, B2b, and M7 sites, and those of the Al(or Si) atom at the M2 site. Relatively small values of N_{out} of Al(or Si) atoms of O1 and B1 may reveal the strong covalent character for the Al(or Si)-*TM* interatomic bonds (O1-O2c or B1-B2c) or the covalent bond formation at the Al(or Si) icosahedron (MI first shell). It should be noted that the charge transfer from Al to the transition metal coexists with the Al(or Si)-*TM* interatomic covalent bond and thus could not be distinguished from each other. Under a rigid-band approximation, Pauling proposed that the $3d$ valence electrons are distributed to the two different kinds of orbitals, atomic orbital (AO) and bonding orbital (BO), in order to explain the composition dependence of the saturation magnetic moment (SMM) in $3d$ transition-metal alloys.[48] The AO shows only weak interatomic interaction and thus causes the SMM. Raynor predicted that in Al-*TM* alloys some of the Al $3s$ and $3p$ electrons are absorbed into the vacancies in AO's of transition metals.[49] This would result in excess valence electrons for transition metals. In addition, $3d$ electrons occupying the BO's of transition metals are distributed in the interatomic region between Al and the transition metal and thus take part in sp-d hybridization. However, we could not distinguish the electrons in the AO's from those in the BO's in our study. Although we could see the charge transfer from Al to transition metal, the sp-d hybridization consequently smears out the charge transfer and gives no meaningful excess valence electrons for transition metals, contrary to the suggestion given by Trambly de Laissardiere *et al.*

From the above considerations, we should interpret the mechanism of pseudogap formation by the combination of the FS-JZ interaction induced by the charge transfer from Al to transition metals, and the enhancement of the covalent bonds. This interpretation can also be reasonably applied to explain the composition dependencies of the Seebeck coefficient and the electrical conductivity of the AlPdRe icosahedral quasicrystal. We have reported recently for the AlPdRe quasicrystal that the Seebeck coefficient reveals a clearer dependence on sample composition than an electrical conductivity.[52] It was found that the Seebeck coefficient rapidly increases with increasing Re or Pd concentration. This behavior can be interpreted as the combination of a charge transfer from Al to Re, and a deepening of the DOS pseudogap by covalent bonds. We have also found that decreasing atomic density with increasing concentrations of Pd and Re might reveal the enhancement of the covalent bonding nature of Al and transition metals.[53]

Finally, we speculate about the possibility of the enhancement of the pseudogap for quasicrystals. In the MI cluster, we did not find that the strength of the covalent bond was similar to all of the 30 bonds for the first shell and all of the 60 bonds for the second shell. In particular, the first shell of the MI cluster indicates interatomic charge density with a

cubic symmetry, which is lower down than icosahedral symmetry, as shown in Fig. 4(a). If we assume that this result arises from the cubic packing nature of the MI cluster, we suppose that for an approximant higher than the 1/1 cubic approximant, the atomic arrangement around the MI cluster approaches the icosahedral environment and then covalent bonds of the MI cluster become isotropically stronger. Consequently, the icosahedral quasicrystal may come to possess a long-range order of the potential waves with icosahedral symmetry thus leading to a deep DOS pseudogap in comparison with the approximant.

In this study, we focused mainly on the discussion about the origin of the DOS pseudogap. However, the number of approximant crystals, which we have obtained with charge density, is still very limited. We are now analyzing powder XRD patterns of the α-AlReSi approximants with various compositions and other crystals such as Al_2Ru and AlCuRu approximants. Details of the composition dependence of bond strength or common features in the bonding nature of the various approximants will be presented in the future. We believe that our study could provide useful information on any physical or chemical phenomena related to chemical bonds in the approximant crystals or quasicrystals. As already known, many Al-based icosahedral quasicrystals are stiffer than other Al-based crystalline alloys. This property may also be attributed to the covalent bonds formed in the icosahedral cluster and the glue atoms. Research along this line needs further detailed charge-density study including study of many other systems of the approximant crystals.

V. CONCLUSION

We successfully obtained the clear images of interatomic covalent bonds between Al and transition metals (Mn, Re) and those in Al(or Si) icosahedron of MI clusters of both α-AlReSi and α-AlMnSi approximant crystals by the MEM/Rietveld method. In particular, Al(or Si)-Re interatomic covalent bonds connecting the first shell with the second shell of MI clusters are the strongest of all the covalent bonds. All three kinds of glue atom are covalently bound to Re or Mn of MI clusters. However, the contribution to the connection of the MI clusters is different from one other: one is connecting the clusters located at both the origin and body center of the unit cell, one is terminating the covalent bonds in the direction of the fivefold axis of the two clusters located at the origin, and another makes no contribution to the connection. This covalent bonding nature should be related to the enhancement of the DOS pseudogap near E_F, thus increasing the electrical resistivity. The charge density at the bond midpoint of Al(or Si)-Re interatomic bonds in α-AlReSi is larger than that in α-AlMnSi. The $5d$ electrons of Re have a stronger hybridization effect or bonding effect than the $3d$ electrons of Mn. In addition, the charge density at the bond midpoint of Al(or Si)-Al(or Si) interatomic bonds in α-AlReSi is also larger than that in α-AlMnSi. This result may arise from the enhancement of the covalent bonding nature of the icosahedron by the stronger termination of the sticking bonds with Re atoms. This fact leads to the low effective carrier density of α-AlReSi in comparison with that of α-AlMnSi. In α-AlReSi and α-AlMnSi, Al atoms of the second shell of the Mackay icosahedron and Al(or Si) atoms of the two glue atom sites, which are only bonded to transition-metal atoms, have a sign of the charge transfer from Al to the transition metal. However, meaningful excess valence electrons for the transition metal were not observed. Unlike the covalent bonding nature of the icosahedron in α-AlReSi and α-AlMnSi crystals, the Al icosahedron with the Re center atom exhibits no Al-Al interatomic covalent bonds in the $Al_{12}Re$ crystal. The tendency for metallic-covalent bonding conversion in Al icosahedron, which is related to the atom site occupancy of the icosahedral cluster center, is also strongly supported.

ACKNOWLEDGMENTS

This work was supported by a Grant-In-Aid for Scientific Research from the Ministry of Education, Science, Sports, and Culture. The synchrotron radiation experiments were performed at the SPring-8 with the approval of the Japan Synchrotron Radiation Research Institute (JASRI).

*Present address: National Institute of Advanced Industrial Science and Technology, Tsukuba, Ibaraki 305-8565, Japan. Electronic address: kz-kirihara@aist.go.jp

[1] K. Kimura and S. Takeuchi, in *Quasicrystals: the State of the Art*, 2nd ed., edited by D. P. Divincezo and P. J. Steinhardt (World Scientific, Singapore, 1999), p. 325.

[2] Ö. Rapp, in *Physical Properties of Quasicrystals*, edited by Z. M. Stadnik (Springer-Verlag, Berlin, 1999), p. 127.

[3] B. D. Biggs, S. J. Poon, and N. R. Munirathnam, Phys. Rev. Lett. **65**, 2700 (1990).

[4] P. Lindqvist, C. Berger, T. Klein, P. Lanco, F. Cyrot-Lackmann, and Y. Calvayrac, Phys. Rev. B **48**, 630 (1993).

[5] R. Haberkern, G. Fritsch, and M. Harting, Appl. Phys. A: Solids Surf. **57**, 431 (1993).

[6] K. Kimura, M. Takeda, M. Fujimori, R. Tamura, H. Matsuda, R. Schmechel, and H. Werheit, J. Solid State Chem. **133**, 302 (1997).

[7] H. Akiyama, Y. Honda, T. Hashimoto, K. Edagawa, and S. Takeuchi, Jpn. J. Appl. Phys., Part 2 **32**, L1003 (1993).

[8] F. S. Pierce, S. J. Poon, and Q. Guo, Science **261**, 737 (1993).

[9] R. Tamura, H. Sawada, K. Kimura, and H. Ino, in *Proceedings of the Sixth International Conference on Quasicrystals*, edited by S. Takeuchi and T. Fujiwara (World Scientific, Singapore, 1998), p. 631.

[10] R. Haberkern, K. Khendri, C. Madel, and P. Haussler, Mater. Sci. Eng., A **294-296**, 475 (2000).

[11] J. J. Préjean, J. C. Lasjaunias, C. Berger, and A. Sulpice, Phys. Rev. B **61**, 9356 (2000).

[12] J. Q. Guo, T. J. Sato, E. Abe, H. Takakura, and A. P. Tsai, Philos. Mag. Lett. **80**, 495 (2000).

[13] I. R. Fisher, X. P. Xie, I. Tudosa, C. W. Gao, C. Song, P. C. Canfield, A. Kracher, K. Dennis, D. Abanoz, and M. J. Kramer, Philos. Mag. B **82**, 1089 (2002).

[14] I. R. Fisher, M. J. Kramer, T. A. Wiener, Z. Islam, A. R. Ross, T.

A. Lograsso, A. Kracher, A. I. Goldman, and P. C. Canfield, Philos. Mag. B **79**, 1673 (1999).
[15] A. Bilušić, Z. Budrović, A. Smontara, J. Dolinšek, P. C. Canfield, and I. R. Fisher, J. Alloys Compd. **342**, 413 (2002).
[16] F. S. Pierce, Q. Guo, and S. J. Poon, Phys. Rev. Lett. **73**, 2220 (1994).
[17] H. Sato, T. Takeuchi, and U. Mizutani, Phys. Rev. B **64**, 094207 (2001).
[18] Y. Yokoyama, A. Tsai, A. Inoue, T. Masumoto, and H. S. Chen, Mater. Trans., JIM **32**, 421 (1991).
[19] T. Fujiwara, Phys. Rev. B **40**, 942 (1989).
[20] M. Krajčí and J. Hafner, Phys. Rev. B **57**, 2849 (1998).
[21] T. Takeuchi, H. Sato, and U. Mizutani, J. Alloys Compd. **342**, 355 (2002).
[22] G. Trambly de Laissardiere, D. Nguyen Manh, L. Magaud, J. P. Julien, F. Cyrot-Lackmann, and D. Mayou, Phys. Rev. B **52**, 7920 (1995).
[23] Z. Dankhazi, G. Trambly de Laissardiere, D. Nguyen Manh, E. Belin, and D. Mayou, J. Phys.: Condens. Matter **5**, 3339 (1993).
[24] E. Belin, J. Kojnok, A. Sadoc, A. Traverse, M. Harmelin, C. Berger, and J. M. Dubois, J. Phys.: Condens. Matter **4**, 1057 (1992).
[25] E. Belin and J. M. Dubois, J. Phys.: Condens. Matter **8**, L717 (1996).
[26] K. Kirihara and K. Kimura, Sci. Technol. Adv. Mater. **1**, 227 (2000).
[27] V. Elser and C. L. Henley, Phys. Rev. Lett. **55**, 2883 (1985).
[28] C. L. Henley and V. Elser, Philos. Mag. B **53**, L59 (1986).
[29] B. D. Biggs, F. S. Pierce, and S. J. Poon, Europhys. Lett. **19**, 415 (1992).
[30] A. Quivy, M. Quiquandon, Y. Calvayrac, F. Faudot, D. Gratias, C. Berger, R. A. Brand, V. Simonet, and F. Hippert, J. Phys.: Condens. Matter **8**, 4223 (1996).
[31] U. Mizutani, T. Takeuchi, and H. Sato, J. Phys.: Condens. Matter **14**, R767 (2002).
[32] R. Tamura, T. Asao, and S. Takeuchi, Phys. Rev. Lett. **86**, 3104 (2001).
[33] R. Tamura, T. Asao, M. Tamura, and S. Takeuchi, Mater. Res. Soc. Symp. Proc. **643**, K13.3.1 (2001).
[34] M. Takata, E. Nishibori, and M. Sakata, Z. Kristallogr. **216**, 71 (2001).
[35] M. Takata, B. Umeda, E. Nishibori, M. Sakata, Y. Saito, M. Ohno, and H. Shinohara, Nature (London) **377**, 46 (1995).
[36] M. Fujimori, T. Nakata, T. Nakayama, E. Nishibori, K. Kimura, M. Takata, and M. Sakata, Phys. Rev. Lett. **82**, 4452 (1999).
[37] M. Takata, E. Nishibori, K. Kato, M. Sakata, and Y. Moritomo, J. Phys. Soc. Jpn. **68**, 2190 (1999).
[38] E. Nishibori, M. Takata, M. Sakata, H. Tanaka, T. Muranaka, and J. Akimitsu, J. Phys. Soc. Jpn. **70**, 2252 (2001).
[39] K. Kirihara, T. Nakata, M. Takata, Y. Kubota, E. Nishibori, K. Kimura, and M. Sakata, Phys. Rev. Lett. **85**, 3468 (2000): Mater. Sci. Eng., A **294-296**, 492 (2000).
[40] E. Nishibori, M. Takata, K. Kato, M. Sakata, Y. Kubota, S. Aoyagi, Y. Kuroiwa, M. Yamakata, and N. Ikeda, Nucl. Instrum. Methods Phys. Res. A **467-468**, 1045 (2001).
[41] P. Villars, *Pearson's Handbook of Crystallographic Data for Intermetallic Phases*, edited by P. Villars and L. D. Calvart (American Society for Metals, Metals Park, OH, 1991), pp. 919 and 990.
[42] H. Tanaka, M. Takata, E. Nishibori, K. Kato, T. Iishi, and M. Sakata, J. Appl. Crystallogr. **35**, 282 (2002).
[43] T. Onogi, T. Takeuchi, H. Sato, and U. Mizutani, J. Alloys Compd. **342**, 397 (2002).
[44] M. Krajčí and J. Hafner, J. Phys.: Condens. Matter **143**, 5755 (2002).
[45] T. Takeuchi, T. Onogi, Y. Sato, and U. Mizutani (private communication).
[46] M. Fujimori and K. Kimura, J. Solid State Chem. **133**, 310 (1997).
[47] A. E. Carlsson, Phys. Rev. B **43**, 12 176 (1991).
[48] L. Pauling, Phys. Rev. **54**, 899 (1938).
[49] G. V. Raynor, Prog. Met. Phys. **1**, 1 (1949).
[50] D. Mayou, F. Cyrot-Lackmann, G. Trambly de Laissardiere, and T. Klein, J. Non-Cryst. Solids **153&154**, 412 (1993).
[51] M. Krajčí, M. Windisch, J. Hafner, G. Kresse, and M. Mihalkovič, Phys. Rev. B **51**, 17 355 (1995).
[52] K. Kirihara and K. Kimura, J. Appl. Phys. **92**, 979 (2002).
[53] K. Kirihara and K. Kimura, Phys. Rev. B **64**, 212201 (2001).